Available online at www.rilem.net

Materials and Structures **38** (March 2005) 267-273

Mechanical response of solid clay brickwork under eccentric loading. Part II: CFRP reinforced masonry

A. Brencich and L. Gambarotta
Department of Structural and Geotechnical Engineering, University of Genoa, Italy

Received: 10 October 2003; accepted: 19 April 2004

ABSTRACT

The mechanical response of solid clay brickwork in presence of CFRP near-surface reinforcement and under eccentric loads is addressed in this paper. Experimental tests on CFRP reinforced masonry (CFRP-RM) prisms under eccentric loads are compared to similar tests on URM specimens in order to give a preliminary insight in the collapse mechanisms of CFRP-reinforced masonry. While URM is found to exhibit a quasi-brittle response, so raising objections to several analytical procedures for masonry bridge assessment, CFRP reinforcement may be responsible of a significant increase in the brickwork compressive strength and ductility. Some considerations on the cracking processes inside reinforced masonry prisms are discussed.

RÉSUMÉ

Dans cette étude, on rapporte les résultats mécaniques d'un mur en briques pleines renforcées superficiellement par des polymères renforcés de fibres de carbone (CFRP) et soumis à des charges excentriques. Les essais expérimentaux sur les murs renforcés par des CFRP soumis à des charges excentriques sont comparables à des essais semblables effectués sur des spécimens URM de façon à fournir des actions préliminaires sur les mécanismes d'effondrement des murs renforcés par des CFRP. Alors que l'URM révèle une réponse presque fragile qui preuve soulever des objections sur les différentes procédures s'analyse pour vérifier les ponts en maçonnerie le renfort avec CFRP peut déterminer une augmentation et de la ductilité des murs. Quelques considérations sur les phénomènes de fissures dans la maçonnerie renforcée sont à examiner.

1. INTRODUCTION

Arches and vaults have been widely used in almost all masonry structures for a long while; only in the last 80 years they have been substituted by r.c. beams and slabs and are now reduced mainly to architectural elements. The degradation of mortar and bricks, due to the atmospheric conditions, and the increase of the service loads make retrofitting and strengthening of arches and vaults a crucial and challenging issue.

Various techniques have been used and tested in the last years; the most popular procedure strengthens arches by means of concrete saddles connected to the arch barrel [1, 2] and by means of a sprayed concrete layer at the arch intrados [2]. Experimental tests proved these technique to be rather effective; objections rise from their cost and from the difficulty in modelling their mechanical effect on the original structure.

Following the same idea of reinforced concrete, some masonry bridges have been retrofitted by near-surface reinforcement, or retro-reinforcement [3, 4], consisting of stainless steel bars grouted at the arch intrados in pre-sawn grooves and anchored in pre-drilled holes. The great advantage of this technique is that traffic does not need to be interrupted, but the efficiency of the grouting material greatly affects the overall structural performances and the strength against delamination of the stainless steel bars.

Recently, glass (GFRP), aramid (AFRP) and carbon (CFRP) fibre reinforced polymers, in the shape of laminates and fabric, rather commonly used to rehabilitate r.c. structures due to their low weight and high strength, have been applied to masonry [5]. The main difference between masonry structures and r.c. beams is that the reinforcement needs to be distributed on the wall rather than concentrated in few and well known areas, as for beams. The main advantages of these materials, *i.e.* low weight, high strength and corrosion resistance, made FRPs to be increasingly used

doi:10.1617/14135

when retrofitting existing structures after earthquakes and upgrading their seismic performance. In particular, FRPs are used to increase the shear strength of walls [5] and their out-of-plane bending resistance [6-9]. The latter case is that of an eccentrically loaded wall with low axial thrust, usually less than 40% of the load carrying capacity of the wall for concentric loading [5]. As different from the strengthened r.c. beams and slabs, the collapse mechanism of FRP-reinforced masonry is seldom due to the detachment of the reinforcement, mainly in the case of GFRPs [7-10]. Experimental tests on reduced scale models of vaults [11] showed that similar collapse mechanisms are found also when the bending moment is coupled with strong axial thrust, that is the case of vaults and arches.

The problem of strengthening masonry arches and vaults, of great importance when retrofitting ancient buildings and masonry arch bridges, is that of an eccentrically loaded wall subjected to out-of-plane bending and relevant axial thrust. In this paper, a series of tests on solid clay brick CFRP-RM specimens is presented and compared to the response of unreinforced masonry [12]. The main collapse mechanisms are discussed and consideration is given to the basic hypotheses on which the standard approaches rely on, among which the plane section hypothesis. Resembling well established approaches [5], an efficient predictive model for the load carrying capacity of the reinforced masonry is presented.

2. SPECIMENS, TEST PROGRAM AND EXPERIMENTAL SETUP

The tested specimens consist of stacks of four 5.5x11x24 cm solid clay bricks with five 10 mm thick mortar (1:1:5) joints and are intended to represent the elementary unit of an arch. They were built at the same time and cured in the same conditions as the URM specimens tested in [12] so as to give a direct estimate of the effect of reinforcement. For the sake of simplicity some data are collected in Table 1; the complete details of the specimens and of the testing apparatus are given in the companion paper [12].

The reinforcement of the specimens has been made by means of the Mitsubishi/Ruredil Replark© system. A plane area on masonry was obtained by a thin layer (2-3 mm thick) of a fiber reinforced cement without shrinkage, Fig. 1 a. The reinforcement, consisting of two parallel strips of Carbon Fiber Reinforced Polymer (CFRP), each one 4 cm wide, was glued by an epoxy resin to the prism and also to the steel plates in order to represent a continuous reinforcement on the whole arch, Fig. 1 b. The amount of reinforcement is rather high because the aim of the research is that of analysing the collapse mechanisms of the reinforced masonry. In what follows, we will assume that the reinforcement never collapses. The mechanical parameters of the CFRP strip are listed in Table 2 as provided by the producer.

Two series of 8 prisms each were produced, for a total amount of 16 prisms, differing only in the composition of mortar (see [12] for details). Each series has been loaded with different eccentricities of 0, 4, 6, 8 and 10 cm both unreinforced (except the 10 cm eccentricity which is too high for URM) and CFRP reinforced (except the

Table 1 - Mechanical parameters for brick and mortar (average values)

BRICK	$E_b = 2400 N/mm^2$	$f_t = 3.4\ N/mm^2$	$f_c = 18.7\ N/mm^2$
MORTAR	$E_m = 335\ N/mm^2$	$f_t = 1.4\ N/mm^2$	$f_c = 14.7\ N/mm^2$

Fig. 1 a - The surface is prepared with a controlled mixture of cement and fillers.

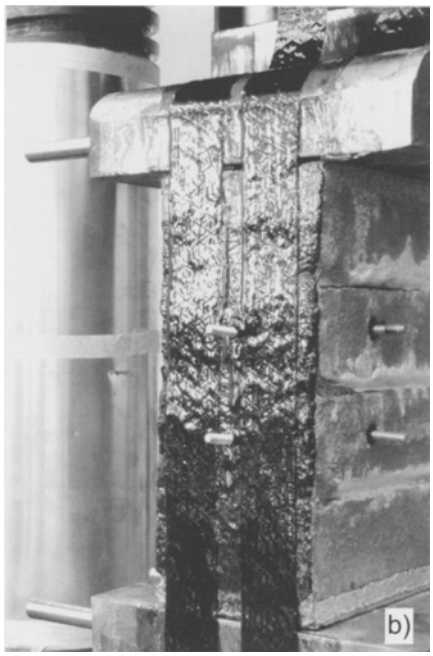

Fig. 1 b - The CFRP strips are glued by epoxy resin.

Table 2 - CFRP reinforcement: mechanical characteristics (Mitsubishi/Ruredil Replark30©)

Thickness	Weight	Elastic modulus	Tensile strength	Ultimate strain
0.167 mm	300 gr/mm^2	>230.000 MPa	>3.400 MPa	>1.3%

concentric load for which no effect can be expected from the reinforcement). The results of the tests on URM specimens are discussed in the companion paper [12] while the tests on CFRP reinforced prisms are discussed below.

3. TEST RESULTS AND COMPARISONS

The load-displacement, load-rotation and moment-rotation response of the reinforced specimens is shown in Fig. 2. Reinforced specimens could be tested also at a 10 cm eccentricity, which has no comparison in URM prisms being this eccentricity too high for testing. It can be seen that a clear linear phase is followed by a softening phase in which inelastic strains are developed and a significant ductility is retained.

Fig. 3 shows the position of the central joint as the load is increased for the 8 and 10 cm eccentricities. The 100% lines stand for the position of the joint at the displacement corresponding to the maximum load, whilst lines referring to over 100% refer to the post-peak phase. It can be seen that the Navier hypothesis of plane section appears to be reasonably verified also in presence of CFRP reinforcement, at least up to the peak load.

The final stage of a CFRP-RM prism is shown in Fig. 4 (e=10 cm). Also in reinforced masonry [12] the compressed part cracks on planes parallel to the external surface. In all the tests masonry crushed in compression; the experimental setup prevented delamination of the CFRP reinforcement.

Figs. 5 and 6 show the direct comparison of the load-displacement and moment-rotation response of URM and CFRP-RM prisms for the 6 cm and 8 cm eccentric loads for both the series. The effect of reinforcement can be recognized as: 1) increasing the specimen strength some 40% for both the eccentricities; 2) ductility is not reduced and, usually, it is enhanced; 3) the stiffness of the specimen remains exactly the same as that of URM prisms. Table 3 summarizes the numerical results of the tests: the ultimate strain is measured at the compressed side of the specimen; the elastic strain is extrapolated from the diagrams as the limit of the linear response and is therefore of uncertain definition for eccentric loading. Differences arising for the 4 cm eccentricity are due to different

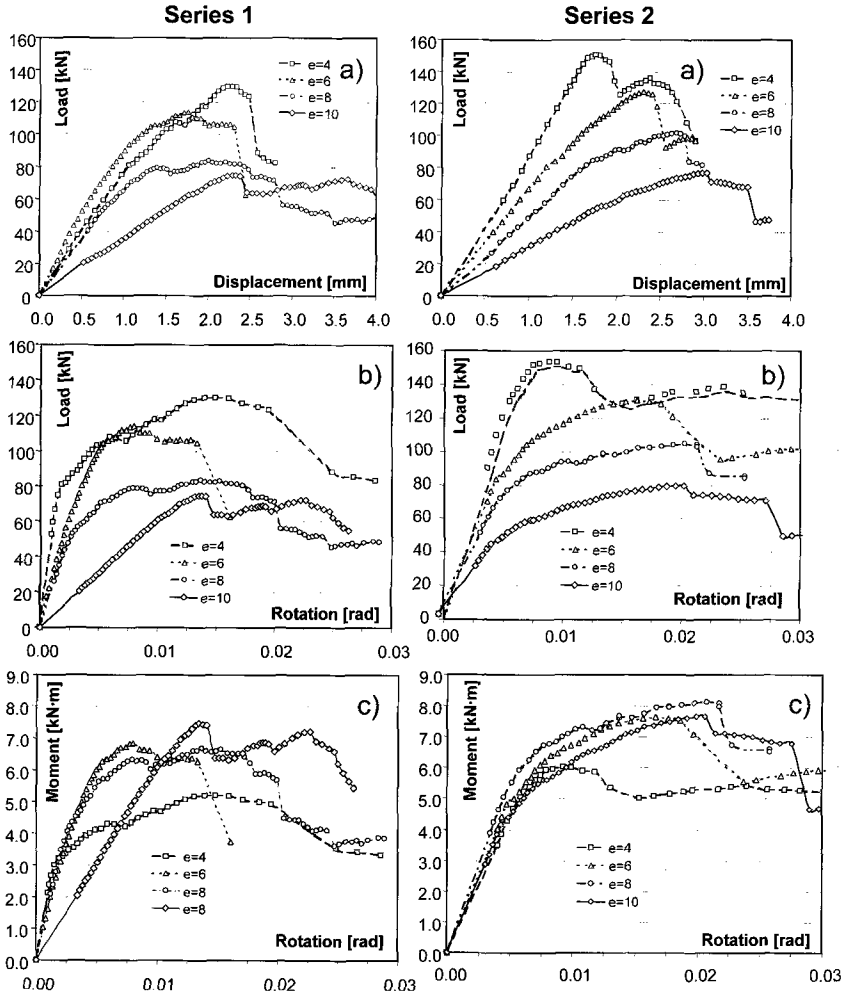

Fig. 2 - a) Load-Displacement, b) Load-Rotation and c) Moment-Rotation curves. Left column: series 1, right column: series 2.

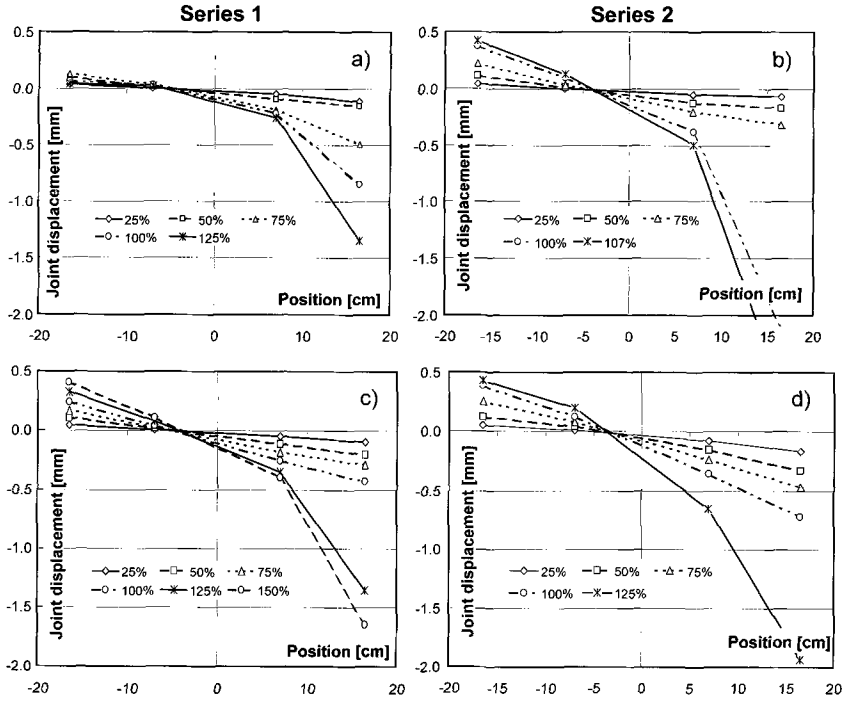

Fig. 3 - Position of the central joint for a) and b) e=8cm and c) and d) e=10cm. Left column: series 1; Right column: series 2.

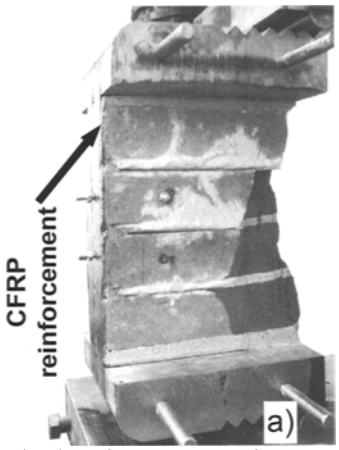

Fig. 4 a - CFRP-RM specimen e=10 cm - series n. 1.

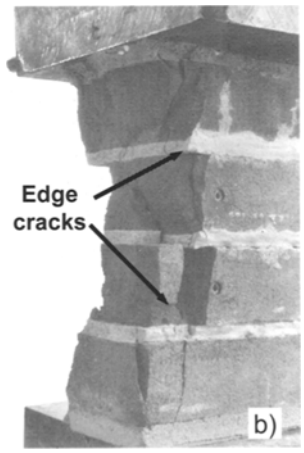

Fig. 4 b - FRP-RM specimen e=10 cm - series n. 1.

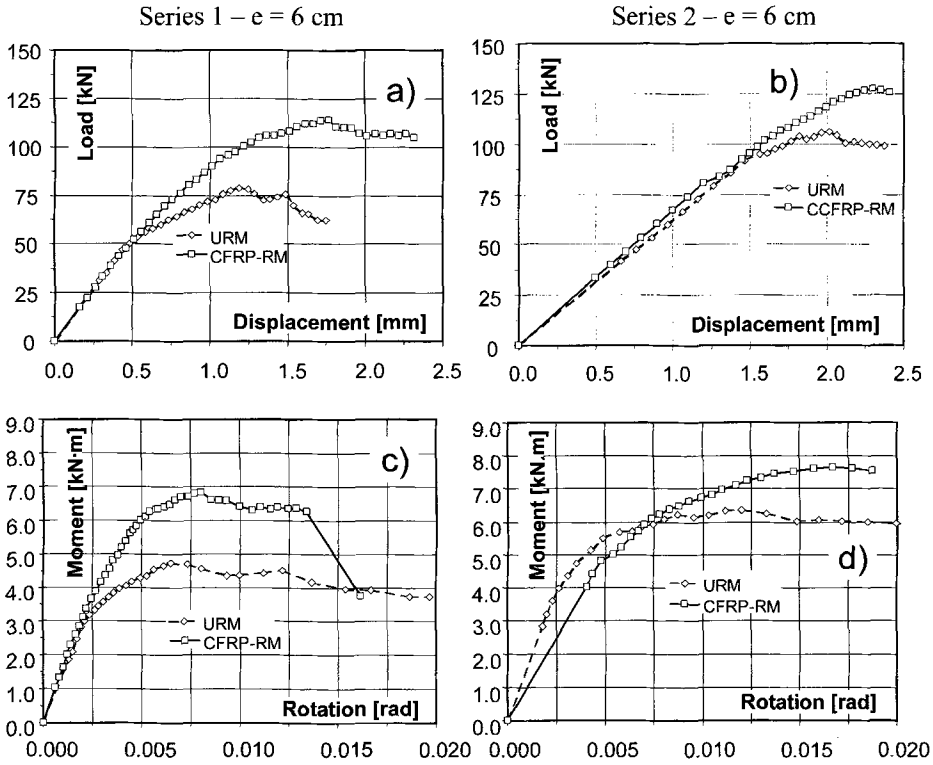

Fig. 5 - CFRP-RM vs. URM response for a 6 cm eccentric load: load-displacement a) and b) and moment-rotation c) and d) curves. Left column: series 1; Right column: series 2.

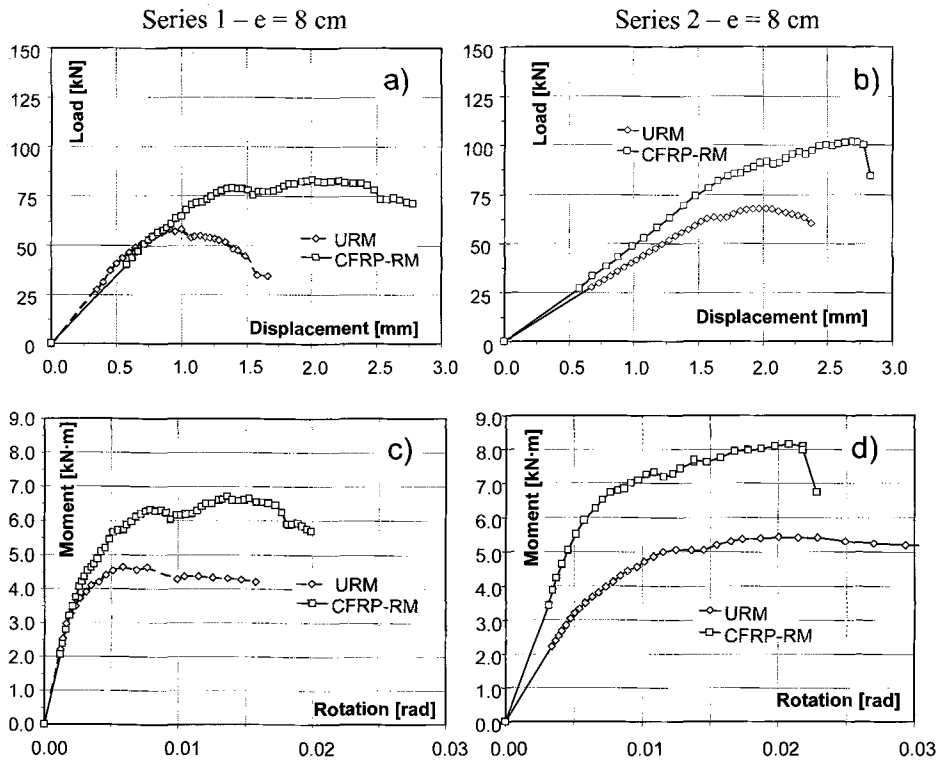

Fig. 6 - CFRP-RM vs. URM response for an 8 cm eccentric load: load-displacement a) and b) and moment-rotation c) and d) curves. Left column: series 1: Right column: series 2.

workmanship since the reinforcement is inefficient for entirely compressed sections.

The ultimate strains for the different eccentricities appear to be rather high. The usual value which is taken into account in theoretical computations for the ultimate strain is 3/1000 [7-9, 13] or 3.5/1000 [5, 13], while the experimental value is here found never less than three times that estimate. This is probably due to the different kind of masonry, which is here a solid clay brickwork while in out-of-plane bending the standard bricks are hollow concrete blocks for the American specimens and perforated modern clay bricks for the latter work [5]. Being the collapse mechanism that of progressive pealing of the compressed side, in the latter case the border effects may be reasonably expected to be much more important than for solid clay brick masonry. Besides, the ultimate strain increases with load eccentricity, which seems in contrast with what was found in [14]; in [14] the bricks were again concrete ones, and the measuring device could also have affected the experimental measurements.

Table 3 - Compressive strength, elastic and ultimate strains and ductility of the concentrically loaded prisms

e		Peak load [kN]		Diff.	El. strain ε_{el} ($*10^3$)		Ul. strain ε_{ul} ($*10^3$)		Ductility δ		Diff.	Series
[cm]		URM	CFRP	%	URM	CFRP	URM	CFRP	URM	CFRP	%	
compress.	0	218	/	-	7.4	/	10.5	/	1.42	/	-	1
		268	/	-	8.8	/	10.7	/	1.20	/	-	2
	4	126	130	+3	6.7	7.8	9.6	9.3	1.43	1.19	-17	1
		156	136	-13	8.1	8.3	9.4	9.7	1.16	1.17	0	2
cracked section	6	75	105	+40	4.2	5.1	6.5	9.1	1.55	1.78	+15	1
		104	127	0	5.5	8.3	8.7	9.1	1.58	1.10	-30	2
	8	58	83	+43	3.4	5.1	5.5	9.2	1.62	1.80	+11	1
		68	102	+50	5.8	6.4	8.8	10.3	1.52	1.61	+6	2
	10	/	75	-	/	8.4	/	14.8	/	1.76	-	1
		/	76	-	/	9.7	/	12.9	/	1.33	-	2

4. AN ANALYTICAL MODEL

The experimental results can be interpreted by means of relatively simple mechanical models. Assuming the classical plane section approach (Navier), a constitutive model for masonry may be that of an elasto-perfectly plastic material limiting the maximum allowable strain to the value found in the tests, Fig. 7. The tensile response is assumed that of a perfectly No-Tensile-Resistance material (NTR), *i.e.* assuming a perfect unilateral contact in compression. The equilibrium equations at collapse are given by:

$$N_{EP} = f'_c by + f'_c b\frac{x-y}{2} + \sigma_{CFRP}A_{CFRP}; \quad (1)$$

$$M_{EP} = N_{EP}e = f'_c by\frac{x-y}{2} + \\ + f'_c b\frac{x-y}{2}\left[(h-y) - \frac{1}{3}(x-y)\right] + \\ + \sigma_{CFRP}A_{CFRP} * e_A \quad (2)$$

where f'_c is the compressive strength for concentric loading, σ_{CFRP} and A_{CFRP} the tensile stress and the net area of the reinforcement, respectively, and other symbols are explained in Fig. 7. Masonry compressive strength is here assumed as independent on the load eccentricity. Once the ultimate strain ε_{ul} is set, the height of the plastic part of the section can be calculated: $y=x(\delta -1)/\delta$. Once the CFRP effective elastic modulus E_{CFRP} is known, the tensile stress may be expressed as $\sigma_{CFRP} = E_{CFRP}\,\varepsilon_{CFRP} = E_{CFRP}\,\varepsilon_{ul}\,(h-x)/x$. Therefore, Equations (1) and (2) may be rewritten as:

$$n = \frac{N_{EP}}{N_0} = \frac{N_{EP}}{f'_c bh} = \frac{x}{h}\frac{2\delta-1}{2\delta} - \\ \rho_{CFRP}\eta\delta\frac{1-x/h}{x/h} \quad (3)$$

$$n\frac{e}{h} = \frac{N_{EP}}{N_0}\frac{e}{h} = \frac{N_{EP}}{f'_c bh}\frac{e}{h} = \\ = \frac{x}{2h}\left[2 - \frac{1}{\delta} + \frac{x}{3h}\left(3 - \delta - \frac{2}{\delta} + \frac{1}{\delta^2}\right)\right] \quad (4)$$

where N_0 stands for the load carrying capacity of the section under concentric loading. In Equations (3) and (4) $\rho_{CFRP} = A_{CFRP}/bh$ stands for the CFRP area fraction and $\eta = E_{CFRP}/E_{MAS}$ is the ratio between the effective elastic modulus of the CFRP and of masonry, a sort of homogenizing ratio. The effective elastic modulus of the CFRP strip takes into account the shear flexibility of the fibre-cement substrate to which the CFRP is glued.

The ultimate limit state set by Equations (3) and (4) allows the limit domain of the masonry section to be represented in a normalized N/N_0-e/h plane, where h stands for the section height, see Fig. 7. In the following, two extreme situations are considered: the response of URM, obtained setting the CFRP area to zero ($A_{CFRP}=0$) in eq. (1), and CFRP-RM sections. assuming i) no ductility ($\delta=1$) and ii) unlimited ductility ($\delta\to\infty$). The URM and CFRP-RM limit domains are represented in Fig. 8, where EP stands for the Elasto-perfectly Plastic model.

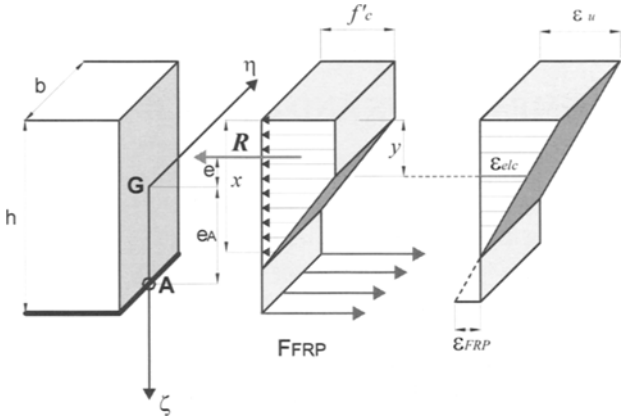

Fig. 7 - Elasto-plastic, No-Tensile-Resistant with ductility control model for the section.

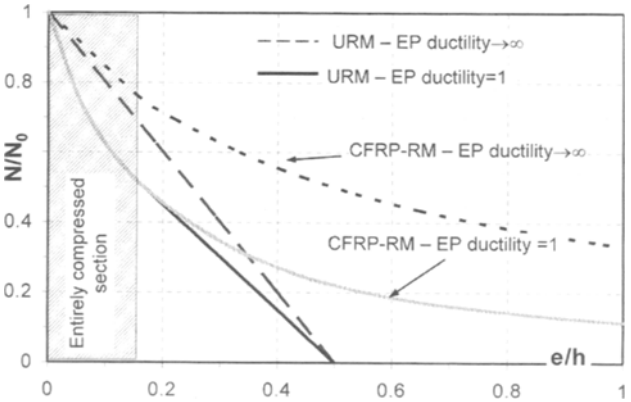

Fig. 8 - Limit N/N_0 – e/h domains for URM and CFRP-RM masonry.

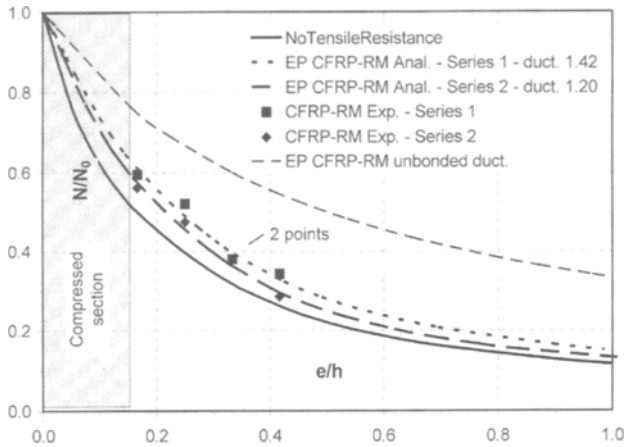

Fig. 9 - Limit domain for CFRP-RM and experimental data.

The domain for CFRP-RM sections for high eccentricities is wider than the URM one, allowing the thrust line to lie outside the section; the greater difference between the two domains is to be found in-between eccentricities e/h ranging from 0.2 to 0.4, *i.e.* for the typical values of the most severe loading conditions on a masonry bridge. Besides, the reinforced section domain is much more sensitive to masonry ductility.

Fig. 9 shows the comparison of the limit curves predicted by Equations (3) and (4) and the experimental data. It can be seen that the relatively simple mechanical models of Fig. 7 fit rather well the experimental points.

5. COMPARISONS AND CONCLUSIONS

A common approach to the eccentric loading of masonry assumes a No Tensile Resistance – Perfectly Brittle (δ=1) constitutive model for brickwork [15]. Under this hypothesis, the compressive strength can be calculated from the limit load through Equations (1) and (2) setting y=0 and A_{CFRP}=0; Table 4 summarizes the estimated values for the compressive strength obtained by means of this approach for the experimental data of this research. It can be observed that the compressive strength of solid clay brick masonry seems not to depend on the load eccentricity. This partially differs from what was found on solid concrete block masonry by other authors [15, 16], but is in agreement with other results [14] and puts forward the need for further experimental and theoretical investigation.

The constitutive model for the section response is somehow more complicate than the standard ULS code-type approach [5, 7-9, 11] which assumes for masonry a No Tensile Resistance model with a stress block distribution in compression, Fig. 10. The stress block height is assumed as a fraction β of the compressed part x, and β is usually assumed equal to 0.8 [5, 11] or 0.85 [7-9] according to an approach which is very close to the classical ULS procedures for r.c. beams. The uniform stress block equivalent to the elastic perfectly-plastic distribution of compressive stresses of Fig. 7 is dependant on the ductility limit δ:

$$\beta = \frac{(2\delta - 1)}{2\delta}. \qquad (5)$$

Fig. 11 plots function (5), showing that the standard values for β, 0.80 or 0.85, would require a ductility δ of 2.5 and 3.33 respectively, far larger than the measured values; assuming for ductility the experimental values of 1.2 and 1.4, the parameter β would be 0.58 and 0.64 respectively. For solid clay brick masonry, the stress block approach needs adequate evaluation of its extension, being the inelastic strains rather low.

Experimental tests showed that CFRP overlay strips may be used to retrofit and strengthen solid clay brick masonry raising its load carrying capacity up to 40% if compared to the URM. Ductility is usually increased, anyway it is never reduced, also in the case of high eccentricity of the axial thrust, typical of the most severe loading conditions on arch-type structures (arches, vaults, masonry bridges). This outcome shows that CFRP near surface reinforcement might be of great efficiency in those cases where a bending reinforcement is needed. Since the load carrying capacity of a masonry arch bridge depends approximately linearly on the load carrying capacity of the section, it can be argued that CFRP reinforcements might significantly increase the load carrying capacity of the whole

Table 4 - Compressive strength of masonry vs. load eccentricity: NTR model

	Series n. 1				Series n. 2			
e [cm]	0	4	6	8	0	4	6	8
f'_c [MPa]	9.9	10.3	9.0	10.6	13.5	14.2	14.0	13.6

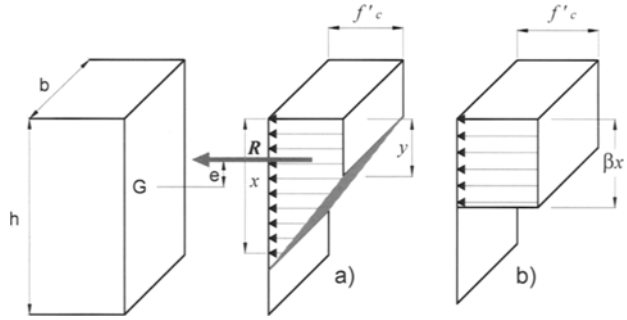

Fig. 10 - Constitutive models for the section: a) elasto-plastic model with ductility limit; b) stress block.

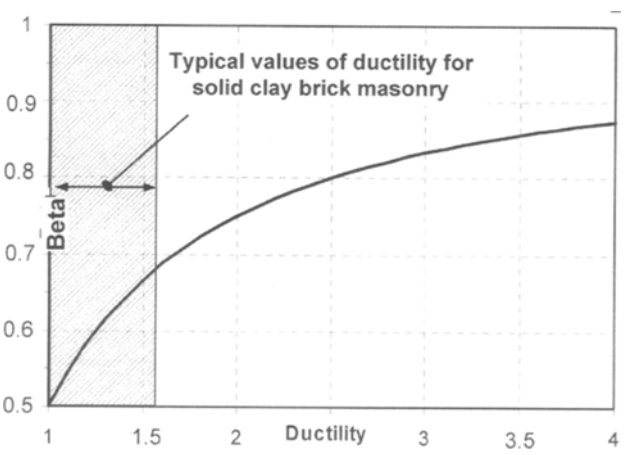

Fig. 11 - Parameter β vs. masonry ductility.

bridge. But too limited experimental results on the reinforcements of masonry structures are available to draw general conclusions.

Further research is needed on the collapse mechanisms and on the effect of CFRP reinforcement of brickwork with different mortars, bricks and of greater thickness.

ACKNOWLEDGEMENTS

The authors acknowledge the contribution by Dott. Giovanni Mantegazza (chair of the Research Dept. - RUREDIL) and Giancarlo Sighieri (Materials Lab. - DISEG) to the experimental work, and the partial financial support of RUREDIL s.p.a., S. Donato Milanese, Italy. This research was carried out also with the partial financial support of the (MURST) Department for University and Scientific and Technological Research in the frame of the PRIN 2002/ 2003 Project "*Safety and Control of Masonry Bridges*".

REFERENCES

[1] Fauchoux, G. and Abdunur, C., 'Strengthening masonry arch bridges through backfill replacement by concrete', Proceedings of the 2nd International Arch Bridge Conference, Sinopoli ed. (Balkema, Rotterdam, 1998) 417-422.

[2] Sumon, S.K., 'Repair and strengthening of five full scale masonry arch bridges', Proceedings of the 2nd International Arch Bridge Conference, Sinopoli ed. (Balkema, Rotterdam, 1998) 407-415.

[3] Falconer, R.E., 'Strengthening masonry arch bridges using stainless steel reinforcement', Proceedings of the 11th International Brick Masonry Conference, Shanghai (1997) 463-483.

[4] Garrity, S.W., 'Near-surface reinforcement of masonry arch highway bridges', Proceedings 9th Canadian Masonry Symposium, Fredericton, (2001).

[5] Triantafillou, T.C., 'Strengthening of masonry structures using epoxy-bonded FRP laminates', *J. Comp. Constr.* **2** (1998) 96-104.

[6] Gilstrap, J.M. and Dolan, C.W., 'Out-of-plane bending of FRP-reinforced masonry walls', *Comp. Sc. and Tech.* **58** (1998) 1277-1284.

[7] Hamilton, H.R. and Dolan, C.W., 'Flexural capacity of glass FRP strengthened concrete masonry walls', *J. Comp. Constr.* **5** (2001) 170-178.

[8] Hamoush, S., McGinley, M., Mlakar, P., Scott, D. and Murray, K., 'Out-of-plane strengthening of masonry walls with reinforced composites', *J. Comp. Constr.* **5** (2001) 139-145.

[9] Hamoush, S., McGinley, M., Mlakar, P. and Terro, M.J., 'Out-of-plane behaviour of surface-reinforced masonry walls', *Constr. Build. Mat.* **16** (2002) 341-351.

[10] Roko, K.E., Boothby, T.E. and Bakis, C.E., 'Strain transfer analysis of masonry prisms reinforced with bonded carbon fiber reinforced polymer sheets', *The Mas. Soc. J.* **19** (2001) 57-68.

[11] Valluzzi, M.R., Valdemarca, M. and Modena, C., 'Behaviour of brick masonry vaults strengthened by FRP laminates', *J. Comp. Constr.* **5** (2001) 163-169.

[12] Brencich, A. and Gambarotta, L., 'Mechanical response of solid clay brickwork under eccentric loading. Part I: Unreinforced masonry', *Mater. Struct.* **38** (276) (2004) 257-266.

[13] Drysdale, R.G., Hamid, A.A. and Baker, L.R., 'Masonry Structures, Behaviour and Design' (Prentice Hall, Englewood Cliffs, 1993).

[14] Maurenbrecher, A.H.P., 'Compressive strength of eccentrically loaded masonry prisms', Proceedings of the 3rd Canadian Masonry Symposium, Edmonton, (1983), 10/1-10/13.

[15] Drysdale, R.G. and Hamid, A.A., 'Capacity of concrete block masonry prisms under eccentric compressive loading', *ACI J.* **80** (June 1979) 707-721.

[16] Hatzinikolas, M., Longworth, J. and Warwaruk, J., 'Failure modes for eccentrically loaded concrete Block masonry walls', *ACI J.* **77** (1980) 258-263.